Nonlinear Dyn (2012) 67:527–540
DOI 10.1007/s11071-011-0003-9

ORIGINAL PAPER

Nonlinear dynamic response of an edge-cracked functionally graded Timoshenko beam under parametric excitation

T. Yan · J. Yang · S. Kitipornchai

Received: 17 November 2009 / Accepted: 27 February 2011 / Published online: 22 March 2011

Abstract This paper investigates the nonlinear flexural dynamic behavior of a clamped Timoshenko beam made of functionally graded materials (FGMs) with an open edge crack under an axial parametric excitation which is a combination of a static compressive force and a harmonic excitation force. Theoretical formulations are based on Timoshenko shear deformable beam theory, von Karman type geometric nonlinearity, and rotational spring model. Hamilton's principle is used to derive the nonlinear partial differential equations which are transformed into nonlinear ordinary differential equation by using the Least Squares method and Galerkin technique. The nonlinear natural frequencies, steady state response, and excitation frequency-amplitude response curves are obtained by employing the Runge–Kutta method and multiple scale method, respectively. A parametric study is conducted to study the effects of material property distribution, crack depth, crack location, excitation frequency, and slenderness ratio on the nonlinear dynamic characteristics of parametrically excited, cracked FGM Timoshenko beams.

T. Yan · S. Kitipornchai
Department of Building and Construction, City University of Hong Kong, Kowloon, Hong Kong, China

J. Yang (✉)
School of Aerospace, Mechanical and Manufacturing Engineering, RMIT University, PO Box 71, Bundoora, VIC 3083 Australia
e-mail: j.yang@rmit.edu.au

Keywords Functionally graded materials · Timoshenko beam · Open edge crack · Parametric excitation · Nonlinear vibration · Frequency response

1 Introduction

Damages in the form of cracks are observed as a result of manufacturing process, fatigue, and heavy dynamic loads, etc. These damages may lead to underdesigned structures in many cases and increase the vulnerability of structures to static and dynamic loads. Although most of these cracked deficient structures are not likely to collapse, they must be limited to designated ultimate loads that should be determined based on the properties of the damaged structure. The dynamic behavior of cracked structures has been a topic of active research over the last few decades. A large number of studies on the free and forced vibration of cracked structures, using analytical or numerical methods or both, are available in open literature [1–8]. For Timoshenko beams in which the effect of transverse shear deformation is nonnegligible, Kisa et al. [9] analyzed the free vibration of cracked Timoshenko beam using a combination of finite element and mode synthesis method. Zheng and Fan [10] developed a modified Fourier series solution technique to calculate the natural frequencies of a Timoshenko beam with an arbitrary number of transverse open cracks. Loya et al. [11] obtained the natural frequencies for flexure vibrations of a cracked Timoshenko beam with simple

boundary conditions. The beam was modeled as two segments connected by an extensional spring and a rotational spring.

Parametric excitation occurs when such system parameters as stiffness, inertia and damping terms vary with time. It is known that an axial force exerted on a beam changes beam stiffness. Hence, a time-varying axial load produces parametric excitation. Unlike forced vibration in which resonance happens when the excitation frequency is equal or close to the natural frequencies of the structure, the response of a parametrically excited system grows as the excitation frequency is twice of the natural frequencies. The parametrically excited structure is governed by a set of Mathieu equations if its axial excitation is harmonic. By taking into account the nonlinear inertia terms, Nayfeh and Pal [12] analyzed the nonlinear vibration of a cantilever beam subjected to parametric excitations. Zavodney and Nayeh [13] derived the nonlinear partial differential equation of a slender cantilever beam carrying a lumped mass at an arbitrary position subjected to a principal parametric excitation. Abou-Rayan et al. [14] obtained nonlinear response of a parametrically excited buckled beam and observed complicated dynamic behaviors such as period-multiplying bifurcations, jump phenomena and chaos. Kar and Dwivedy [15] dealt with the nonlinear behavior of a beam with a principal parametric resonance of its first mode and a 3:1 internal resonance between its first two modes. Anderson et al. [16] experimentally investigated the planar responses of a parametrically excited, inextensional slender cantilever beam based on the analytical model in which a quadratic damping was added. The experimental results were in good agreement with the theoretically predicted ones.

Functionally graded materials (FGMs) have attracted increasing research efforts over the past few years due to their outstanding properties. Numerous studies on the dynamic behavior and fracture of FGM structures have been reported [17–30]. Investigations concerning the effect of crack defects on the dynamic behavior of FGM structures haven also received increasing attention recently. Sridhar et al. [31] analyzed wave propagation in FGM beams and layered structures containing embedded horizontal or vertical edge cracks using pseudospectral finite element method. Yang and Chen analytically discussed the influence of open edge cracks on the free and forced linear vibration of FGM beams under an axial force and a moving

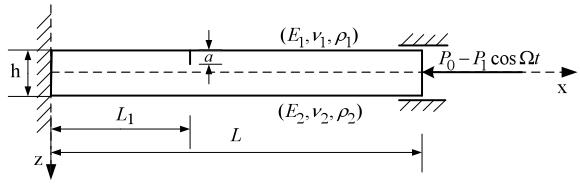

Fig. 1 A clamped FGM beam with an open edge crack under axial excitation

load [32] and the elastic stability characteristics of an Euler–Bernoulli FGM beam with different boundary conditions [33]. Ke et al. [34] studied the flexural vibration and elastic buckling of a cracked FGM Timoshenko beam.

It should be noted that the above investigations [31–34] are based on linear beam theory and do not account for the nonlinear deformation, which may give unreasonable results for FGM beams undergoing nonlinear vibrations when subjected to large external dynamic loads. Most recently, Yang et al. [35] investigated the nonlinear dynamic response of a functionally graded plate with a through-width surface crack. This paper presents analytical solutions for the nonlinear free and forced vibrations of clamped FGM beams with an open edge crack under axial parametric excitation by using Timoshenko beam theory, von-Karman type geometric nonlinearity, and rotational spring model. The nonlinear natural frequencies, steady state deflection response and excitation frequency-amplitude characteristics have been obtained. Comprehensive numerical results are provided to study the effects of material property gradient, crack depth, crack location, excitation frequency, and slenderness ratio on the nonlinear dynamic behavior of cracked FGM Timoshenko beams.

2 The rotational spring model

Figure 1 shows a clamped FGM Timoshenko beam of length L, width b, thickness h, and containing an open edge crack of depth a located at a distance L_1 from the left end. The beam is movable in the longitudinal direction at the right end when subjected to a combine action $P = P_0 - P_1 \cos \Omega t$ which consists of a static compressive force P_0 and a dynamic force $P_1 \cos \Omega t$ with magnitude of P_1 and excitation frequency Ω. These forces are positive for compressive and negative for tensile. The Young's modulus $E(z)$, shear modulus

$\mu(z)$ and mass density $\rho(z)$ of the beam vary exponentially in the thickness direction according to

$$E(z) = E_0 e^{\beta z}, \quad \mu(z) = \mu_0 e^{\beta z}, \quad \rho(z) = \rho_0 e^{\beta z} \tag{1}$$

where E_0, μ_0, and ρ_0 are the Young's modulus, shear modulus, and mass density at the midplane ($z = 0$) of the beam. β is a constant describing the material property gradient along the thickness direction, and $\beta = 0$ corresponds to an isotropic homogeneous beam. Poisson's ratio ν is taken as a constant ($\nu_1 = \nu_2 = \nu$) in the analysis since its influence on the stress intensity factors (SIFs) is quite limited [20].

It is assumed that the crack is perpendicular to the beam surface and always remains open. The well-accepted rotational spring model can then be used to treat the cracked beam as two subbeams connected by a massless elastic rotational spring at the cracked section whose flexibility due to the edge crack can be derived from [36]

$$\frac{1-\nu^2}{E(a)} K_I^2 = \frac{M_I^2}{2} \frac{dG}{da} \tag{2}$$

where M_I is the bending moment at the cracked section. K_I is the SIF under mode I bending load. $E(a)$ is Young's modulus at the crack tip. Based on the data given by Erdogan and Wu [20], the magnitude of SIF, which is a function of dimensionless crack depth $\varsigma = \frac{a}{h}$, can be obtained by using Lagrange interpolation technique as detailed in our previous study [34].

3 Governing equations

Let the longitudinal displacement and transverse deflection of an arbitrary point of the beam be denoted by $\bar{u}(x, z, t)$ and $\bar{w}(x, z, t)$, respectively. Timoshenko beam theory gives

$$\bar{u}(x, z, t) = u(x, t) - z\varphi(x, t), \tag{3a}$$

$$\bar{w}(x, z, t) = w(x, t) \tag{3b}$$

where $u(x, t)$ and $w(x, t)$ are displacement components in the midplane, $\varphi(x, t)$ is the cross-section rotation, and t is time.

By using Hamilton's principle, the governing differential equations of motion of the beam can be derived as

$$\frac{\partial N}{\partial x} = I_0 \frac{\partial^2 u}{\partial t^2} - I_1 \frac{\partial^2 \varphi}{\partial t^2}, \tag{4a}$$

$$\frac{\partial Q}{\partial x} + \frac{\partial}{\partial x}\left(N \frac{\partial w}{\partial x}\right) = I_0 \frac{\partial^2 w}{\partial t^2} + P\left(\frac{\partial^2 w}{\partial x^2}\right), \tag{4b}$$

$$\frac{\partial M}{\partial x} - Q = I_1 \frac{\partial^2 u}{\partial t^2} - I_2 \frac{\partial^2 \varphi}{\partial t^2} \tag{4c}$$

where the inertia terms (I_0, I_1, I_2), axial force N, shear force Q, and bending moment M are defined as

$$\begin{aligned} &(I_0, I_1, I_2) = b \int_{-h/2}^{h/2} \rho(z)\left(1, z, z^2\right) dz; \\ &\begin{bmatrix} N \\ M \end{bmatrix} = \begin{bmatrix} A_{11} & B_{11} \\ B_{11} & D_{11} \end{bmatrix} \begin{bmatrix} \frac{\partial u}{\partial x} + \frac{1}{2}\left(\frac{\partial w}{\partial x}\right)^2 \\ -\frac{\partial \varphi}{\partial x} \end{bmatrix}, \\ &Q = \kappa_s E_{44}\left(\frac{\partial w}{\partial x} - \varphi\right) \end{aligned} \tag{5}$$

where the shear correction factor $\kappa_s = 5/6$ and the stiffness elements of the beam are

$$\begin{aligned} &(A_{11}, B_{11}, D_{11}) = b \int_{-h/2}^{h/2} \frac{E(z)}{1-\nu^2}\left(1, z, z^2\right) dz, \\ &E_{44} = b \int_{-h/2}^{h/2} \mu(z)\, dz \end{aligned} \tag{6}$$

For the cracked FGM beam considered in the present analysis, the boundary conditions require

$$u_1 = 0, \quad w_1 = 0, \quad \varphi_1 = 0 \quad \text{at } x = 0, \tag{7a}$$

$$N_2 = 0, \quad w_2 = 0, \quad \varphi_2 = 0 \quad \text{at } x = L \tag{7b}$$

At the cracked section ($x = L_1$), the compatibility conditions enforce the continuities of the axial displacement, transverse deflection, axial force, bending moment, and shear force across the crack. The discontinuity in the slope is proportional to the bending moment transmitted by the cracked section. Thus, we have

$$u_1 = u_2, \quad w_1 = w_2, \tag{8a}$$

$$\begin{aligned} &N_1 = N_2, \quad M_1 = M_2, \\ &Q_1 - P\frac{\partial w_1}{\partial x} = Q_2 - P\frac{\partial w_2}{\partial x}, \end{aligned} \tag{8b}$$

$$k_T(\varphi_1 - \varphi_2) = M_1 \tag{8c}$$

In (7a, 7b) and (8a, 8b, 8c), subscript $i = 1$, and $i = 2$ refer to the left subbeam and right subbeam divided by an open edge crack.

4 Linear free vibration analysis

We first consider the linear free vibration of a cracked FGM beam subjected to a static compressive force $P = P_0$. Neglecting the axial inertia term and the nonlinear part in (5), then substituting this equation into (4a, 4b, 4c) yields the linear governing equations of motion for the ith subbeam

$$A_{11}\frac{\partial^2 u_i}{\partial x^2} - B_{11}\frac{\partial^2 \varphi_i}{\partial x^2} = -I_1\frac{\partial^2 \varphi_i}{\partial t^2}, \tag{9a}$$

$$\kappa_s E_{44}\left(\frac{\partial^2 w_i}{\partial x^2} - \frac{\partial \varphi_i}{\partial x}\right) = I_0\frac{\partial^2 w_i}{\partial t^2} + P_0\frac{\partial^2 w_i}{\partial x^2}, \tag{9b}$$

$$B_{11}\frac{\partial^2 u_i}{\partial x^2} - D_{11}\frac{\partial^2 \varphi_i}{\partial x^2} - \kappa_s E_{44}\left(\frac{\partial w_i}{\partial x} - \varphi_i\right) = -I_2\frac{\partial^2 \varphi_i}{\partial t^2} \tag{9c}$$

Let ω be the natural frequency of the cracked beam, λ be its dimensionless form, A_0 and I denote the A_{11} and I_0 of an intact homogeneous beam, respectively. With the use of following dimensionless quantities:

$$\begin{aligned}
&(p, p_0, p_1) = (P, P_0, P_1)/A_0, \quad e_{44} = \kappa_s E_{44}/A_0,\\
&\tilde{U}_i = u_i/L, \quad \tilde{W}_i = w_i/L, \quad \tilde{\varphi}_i = \varphi_i,\\
&\xi = x/L, \quad \Delta = L_1/L, \quad a_{11} = A_{11}/A_0,\\
&b_{11} = B_{11}/A_0 L, \quad d_{11} = D_{11}/A_0 L^2,\\
&\bar{I}_0 = I_0/I, \quad \bar{I}_1 = I_1/IL, \quad \bar{I}_2 = I_2/IL^2,\\
&\bar{t} = t\sqrt{A_0/IL^2}, \quad (\lambda, \bar{\Omega}) = (\omega, \Omega)\sqrt{IL^2/A_0}
\end{aligned} \tag{10}$$

Equations (9a, 9b, 9c) can be rewritten in dimensionless form as

$$a_{11}\frac{\partial^2 \tilde{U}_i}{\partial \xi^2} - b_{11}\frac{\partial^2 \tilde{\varphi}_i}{\partial \xi^2} = -\bar{I}_1\frac{\partial^2 \tilde{\varphi}_i}{\partial \bar{t}^2} \tag{11a}$$

$$e_{44}\left(\frac{\partial^2 \tilde{W}_i}{\partial \xi^2} - \frac{\partial \tilde{\varphi}_i}{\partial \xi}\right) = \bar{I}_0\frac{\partial^2 \tilde{W}_i}{\partial \bar{t}^2} + p_0\frac{\partial^2 \tilde{W}_i}{\partial \xi^2} \tag{11b}$$

$$b_{11}\frac{\partial^2 \tilde{U}_i}{\partial \xi^2} - d_{11}\frac{\partial^2 \tilde{\varphi}_i}{\partial \xi^2} - e_{44}\left(\frac{\partial \tilde{W}_i}{\partial \xi} - \tilde{\varphi}_i\right) = -\bar{I}_2\frac{\partial^2 \tilde{\varphi}_i}{\partial \bar{t}^2} \tag{11c}$$

Accordingly, the boundary conditions (7a, 7b) become

$$\tilde{U}_1 = 0, \quad \tilde{W}_1 = 0, \quad \tilde{\varphi}_1 = 0 \quad \text{at } \xi = 0 \tag{12a}$$

$$\tilde{N}_2 = 0, \quad \tilde{W}_2 = 0, \quad \tilde{\varphi}_2 = 0 \quad \text{at } \xi = 1 \tag{12b}$$

and the compatibility conditions (8a, 8b, 8c) can be nondimensionalized as

$$\tilde{U}_1 = \tilde{U}_2, \quad \tilde{W}_1 = \tilde{W}_2, \tag{13a}$$

$$\tilde{N}_1 = \tilde{N}_2, \quad \tilde{M}_1 = \tilde{M}_2,$$

$$\tilde{Q}_1 - p_0\frac{\partial \tilde{W}_1}{\partial \xi} = \tilde{Q}_2 - p_0\frac{\partial \tilde{W}_2}{\partial \xi}, \tag{13b}$$

$$k_T(\tilde{\varphi}_1 - \tilde{\varphi}_2) = \tilde{M}_1 \tag{13c}$$

where $\tilde{N}_i$, $\tilde{Q}_i$, $\tilde{M}_i$ $(i = 1, 2)$ are the dimensionless axial forces, shear forces, and bending moments.

For harmonic vibration, it can be assumed that

$$\tilde{U}_i(\xi, \bar{t}) = U_i(\xi)e^{i\lambda\bar{t}}, \tag{14a}$$

$$\tilde{W}_i(\xi, \bar{t}) = W_i(\xi)e^{i\lambda\bar{t}}, \tag{14b}$$

$$\tilde{\varphi}_i(\xi, \bar{t}) = \Phi_i(\xi)e^{i\lambda\bar{t}} \tag{14c}$$

Substituting (14a, 14b, 14c) into (11a, 11b, 11c) leads to a set of ordinary differential equations in λ whose solutions can be readily obtained as

$$\begin{aligned}
U_i = &\left(-m_1\alpha - \frac{n_1}{\alpha}\right)e_{i1}\cos(\alpha\xi)\\
&+ \left(m_1\alpha + \frac{n_1}{\alpha}\right)e_{i2}\sin(\alpha\xi)\\
&+ \left(-m_1\beta + \frac{n_1}{\beta}\right)e_{i3}\cosh(\beta\xi)\\
&+ \left(-m_1\beta + \frac{n_1}{\beta}\right)e_{i4}\sinh(\beta\xi)\\
&+ g_i\xi + g_{i0}
\end{aligned} \tag{15a}$$

$$W_i = e_{i1}\sin(\alpha\xi) + e_{i2}\cos(\alpha\xi) + e_{i3}\sinh(\beta\xi) + e_{i4}\cosh(\beta\xi) \tag{15b}$$

$$\begin{aligned}
\Phi_i = &\left(-m\alpha^3 + n\alpha\right)e_{i1}\cos(\alpha\xi)\\
&+ \left(m\alpha^3 - n\alpha\right)e_{i2}\sin(\alpha\xi)\\
&+ \left(m\beta^3 + n\beta\right)e_{i3}\cosh(\beta\xi)\\
&+ \left(m\beta^3 + n\beta\right)e_{i4}\sinh(\beta\xi)
\end{aligned} \tag{15c}$$

where

$$d = d_{11} - \frac{b_{11}^2}{a_{11}}, \quad c_1 = d\left(1 - \frac{p_0}{e_{44}}\right),$$

$$c_2 = \frac{-d\lambda^2 \bar{I}_0}{e_{44}} + \left(\frac{\bar{I}_1\lambda^2 b_{11}}{a_{11}} + e_{44} - \lambda^2 \bar{I}_2\right)\left(1 - \frac{p_0}{e_{44}}\right) - e_{44},$$

$$c_3 = \frac{(\frac{\bar{I}_1\lambda^2 b_{11}}{a_{11}} + e_{44} - \lambda^2 \bar{I}_2)\lambda^2 \bar{I}_0}{e_{44}},$$

$$\alpha = \sqrt{\frac{\sqrt{c_2^2 + 4c_1c_3} - c_2}{2c_1}},$$

$$\beta = \sqrt{\frac{\sqrt{c_2^2 + 4c_1c_3} + c_2}{2c_1}},$$

$$m = \frac{c_1}{\frac{\bar{I}_1\lambda^2 b_{11}}{a_{11}} + e_{44} - \lambda^2 \bar{I}_2},$$

$$m_1 = \frac{(d_{11}\bar{I}_1\lambda^2 - b_{11}\bar{I}_2\lambda^2 + b_{11}e_{44})(\frac{p_0}{e_{44}} - 1)}{b_{11}\bar{I}_1\lambda^2 - a_{11}\bar{I}_2\lambda^2 + a_{11}e_{44}},$$

$$n = \frac{e_{44} + \frac{d\lambda^2 \bar{I}_0}{e_{44}}}{\frac{\bar{I}_1\lambda^2 b_{11}}{a_{11}} + e_{44} - \lambda^2 \bar{I}_2},$$

$$n_1 = \frac{e_{44}\bar{I}_1\lambda^2 + \frac{(d_{11}\bar{I}_1\bar{I}_0\lambda^4 + b_{11}e_{44}\bar{I}_0\lambda^2 - b_{11}\bar{I}_0\bar{I}_2\lambda^4)}{e_{44}}}{b_{11}\bar{I}_1\lambda^2 - a_{11}\bar{I}_2\lambda^2 + a_{11}e_{44}}$$

Note that e_{ij}, g_i, g_{i0} $(i = 1, 2;\ j = 1, \ldots, 4)$ are constants to be determined from boundary conditions and the compatibility conditions at the cracked section given in (12) and (13). This gives a set of nonlinear homogeneous equations whose determinant should be zero for a nontrivial solution

$$\det[H(\lambda)] = 0 \tag{16}$$

The linear natural frequencies and the associated mode shapes of the cracked FGM beam can then be obtained by solving (16). The expression of this determinant is given in Appendix.

5 Parametrically excited vibration analysis

5.1 Nonlinear governing equations

We now turn our attention to the nonlinear vibration analysis of cracked FGM beams under parametric excitation which contains both static and dynamic axial forces. Substituting (5) into (4), neglecting axial inertia term and using the dimensionless quantities defined in (10) yields the dimensionless nonlinear equations of motion

$$a_{11}\left(\frac{\partial^2 \tilde{U}}{\partial \xi^2} + \frac{\partial \tilde{W}}{\partial \xi}\frac{\partial^2 \tilde{W}}{\partial \xi^2}\right) - b_{11}\frac{\partial^2 \tilde{\varphi}}{\partial \xi^2} = -I_1\frac{\partial^2 \tilde{\varphi}}{\partial \bar{t}^2} \tag{17a}$$

$$e_{44}\left(\frac{\partial^2 \tilde{W}}{\partial \xi^2} - \frac{\partial \tilde{\varphi}}{\partial \xi}\right) + a_{11}\frac{\partial}{\partial \xi}\left(\frac{\partial \tilde{U}}{\partial \xi}\frac{\partial \tilde{W}}{\partial \xi}\right) + \frac{3}{2}a_{11}\left(\frac{\partial \tilde{W}}{\partial \xi}\right)^2\frac{\partial^2 \tilde{W}}{\partial \xi^2} - b_{11}\frac{\partial}{\partial \xi}\left(\frac{\partial \tilde{\varphi}}{\partial \xi}\frac{\partial \tilde{W}}{\partial \xi}\right) - (p_0 - p_1\cos\bar{\Omega}\bar{t})\frac{\partial^2 \tilde{W}}{\partial \xi^2} = \bar{I}_0\frac{\partial^2 \tilde{W}}{\partial \bar{t}^2} \tag{17b}$$

$$b_{11}\left(\frac{\partial^2 \tilde{U}}{\partial \xi^2} + \frac{\partial \tilde{W}}{\partial \xi}\frac{\partial^2 \tilde{W}}{\partial \xi^2}\right) - d_{11}\frac{\partial^2 \tilde{\varphi}}{\partial \xi^2} - e_{44}\left(\frac{\partial \tilde{W}}{\partial \xi} - \tilde{\varphi}\right) = -\bar{I}_2\frac{\partial^2 \tilde{\varphi}}{\partial \bar{t}^2} \tag{17c}$$

Using single mode approximation, the dynamic deformation components for the ith subbeam can be expressed in the following form:

$$\left(\tilde{U}_i, \tilde{W}_i, \tilde{\varphi}_i\right) = \left(r_i^U U_i(\xi), r_i^W W_i(\xi), r_i^\Phi \Phi_i(\xi)\right)q(\bar{t}) \quad (i = 1, 2) \tag{18}$$

where $q(\bar{t})$ is the function of $\bar{t}$ to be determined, r_i^U, r_i^W, r_i^Φ are the unknown constants, and mode shape functions U_i, W_i, Φ_i are given in (15).

Substituting (18) into nonlinear boundary and compatibility conditions, expressing the total squared residual in terms of coefficients r_i^U, r_i^W, r_i^Φ, and then applying the least squares technique to minimize the residual E_{rr} gives

$$\frac{\partial E_{rr}}{\partial r_i^U} = 0, \qquad \frac{\partial E_{rr}}{\partial r_i^\Phi} = 0 \tag{19}$$

This results in a set of homogeneous equations in r_i^U, r_i^W, r_i^Φ that can be used to express r_i^U and r_i^Φ by r_i^W. Reexpressing (18) in terms of r_i^W and putting it into (17) and applying Galerkin integration yields the following nonlinear dynamic governing equation

$$\ddot{q} + \left(k_1 + k_2 p_1\cos\bar{\Omega}\bar{t}\right)q + k_3 q^2 + k_4 q^3 = 0 \tag{20}$$

In order to dissipate the influence of free vibration to get steady state response, a damping term is added to (20)

$$\ddot{q} + a_1\dot{q} + \left(k_1 + k_2 p_1\cos\bar{\Omega}\bar{t}\right)q + k_3 q^2 + k_4 q^3 = 0 \tag{21}$$

Table 1 Coefficients k_1, k_2, k_3, k_4 of cracked FGM beams with $E_2/E_1 = 5.0$

Crack location L_1/L	Crack depth a/h	k_1	k_2	k_3	k_4
0.0	0.1	0.1519	4.947	−0.005612	2.9630
	0.3	0.1243	4.641	−0.001189	0.2495
	0.5	0.1028	4.595	−0.0004896	0.0887
0.1	0.1	0.1564	5.080	−0.0007773	0.0669
	0.3	0.1473	5.253	0.0007613	0.0670
	0.5	0.1371	5.467	−0.0005038	0.0682
0.2	0.1	0.1582	5.075	−0.0004678	0.0244
	0.3	0.1597	5.320	0.0004969	0.0366
	0.5	0.1655	5.811	−0.0006145	0.0490
0.3	0.1	0.1575	4.982	0.0005220	0.0273
	0.3	0.1543	4.469	−0.0004770	0.0233
	0.5	0.1579	3.002	−0.0001749	0.0028
0.4	0.1	0.1566	4.884	−0.0008914	0.0878
	0.3	0.1484	3.762	−0.0005381	0.0927
	0.5	0.1372	1.790	0.0004897	0.0943
0.5	0.1	0.1562	4.847	−26.41	0.1087e6
	0.3	0.1449	3.574	−12.25	0.1189e5
	0.5	0.1264	1.577	−2.740	1580

where a_1 is the damping coefficient, an over dot denotes differentiation with respect to time. Constants k_i $(i = 1 \sim 4)$ are directly dependent on the depth and location of the crack, the axial static compressive load and beam parameters such as material property gradient and beam geometry. Tables 1, 2, 3 list their values at $E_2/E_1 = 0.2, 1.0, 5.0$, $a/h = 0.1, 0.3, 0.5$, $L_1/L = 0.0, 0.1, 0.2, 0.3, 0.4, 0.5$, and $L/h = 6$. Here, E_1 and E_2 denote Young's modulus at the top and bottom surfaces of the beam, respectively. $E_2/E_1 = 1.0$ corresponds to a special case where the beam is isotropic homogeneous. As can be seen, the constant showing the effect of parametric excitation, k_2, increases as E_2/E_1 decreases from 5.0 to 0.2. At same E_2/E_1 ratio, k_2 decreases as the crack depth grows when the crack is located at $L_1/L = 0.0, 0.3, 0.4, 0.5$ whereas increases at $L_1/L = 0.1, 0.2$. k_1 and k_3 are related to the inhomogeneous material properties and k_3 is zero for homogeneous beams $(E_2/E_1 = 1.0)$ that do not have bending-stretching coupling effect. k_4 describes the influence of nonlinear bending deformation.

The nonlinear natural frequency can be obtained from (20) and the steady state response is calculated by solving (21) with the Runge–Kutta method.

5.2 Frequency response

To find the approximate solution of frequency-amplitude response from (20), multiple scale method is employed in this study, beginning by introducing a dimensionless small perturbation parameter ε to serve as a measure of the amplitude. Applying the following scale transforms to (21),

$$a_1 \to \varepsilon a_1, \quad k_l \to \varepsilon k_l, \quad l = 2 \sim 4 \tag{22}$$

one has

$$\ddot{q} + \varepsilon a_1 \dot{q} + \left(k_1 + \varepsilon k_2 p_1 \cos \bar{\Omega} t\right) q + \varepsilon k_3 q^2 + \varepsilon k_4 q^3 = 0 \tag{23}$$

Then two time scales $T = \bar{t}$, $\tau = \varepsilon \bar{t}$ are chosen to seek the approximation of the expansion

$$q(\bar{t}, \varepsilon) = q_0(T, \tau) + \varepsilon q_1(T, \tau) + \cdots \tag{24}$$

The first- and second-order differential operators become

$$\frac{d}{d\bar{t}} = D_0 + \varepsilon D_1, \tag{25a}$$

Table 2 Coefficients k_1, k_2, k_3, k_4 of cracked FGM beams with $E_2/E_1 = 1.0$

Crack location L_1/L	Crack depth a/h	k_1	k_2	k_4
0.0	0.1	0.1636	12.16	1.9410
	0.3	0.1284	11.41	0.1718
	0.5	0.1067	11.45	0.0784
0.1	0.1	0.1707	12.59	0.0718
	0.3	0.1584	13.17	0.0725
	0.5	0.1468	13.76	0.0753
0.2	0.1	0.1736	12.61	0.0338
	0.3	0.1763	13.48	0.0427
	0.5	0.1879	15.09	0.0617
0.3	0.1	0.1725	12.27	0.0337
	0.3	0.1687	10.30	0.0204
	0.5	0.1855	4.936	−0.0131
0.4	0.1	0.1711	11.90	0.0965
	0.3	0.1604	7.999	0.1060
	0.5	0.1448	2.148	0.0770
0.5	0.1	0.1705	11.78	84.70
	0.3	0.1545	7.452	6910
	0.5	0.1297	1.725	43790

Table 3 Coefficients k_1, k_2, k_3, k_4 of cracked FGM beams with $E_2/E_1 = 0.2$

Crack location L_1/L	Crack depth a/h	k_1	k_2	k_3	k_4
0.0	0.1	0.1472	24.39	−0.003544	1.6380
	0.3	0.1108	22.98	−0.0006342	0.1225
	0.5	0.0924	23.17	0.0003940	0.0636
0.1	0.1	0.1550	25.48	−0.0006890	0.0672
	0.3	0.1414	26.88	0.0006423	0.0675
	0.5	0.1304	28.05	−0.0004508	0.0698
0.2	0.1	0.1583	25.53	0.0004856	0.0295
	0.3	0.1621	27.82	0.0005691	0.0427
	0.5	0.1772	31.64	−0.0004933	0.0646
0.3	0.1	0.1571	24.61	0.0004715	0.0293
	0.3	0.1537	19.01	−0.0003378	0.0136
	0.5	0.1759	5.393	−0.0006384	−0.0355
0.4	0.1	0.1554	23.75	−0.0009120	0.0883
	0.3	0.1426	13.54	−0.0001299	0.0986
	0.5	0.1236	0.677	−0.0001068	0.0047
0.5	0.1	0.1547	23.46	−27.67	74960
	0.3	0.1352	12.38	−5.062	3571
	0.5	0.1080	−0.055	−0.02963	6.020

$$\frac{d^2}{d\bar{t}^2} = D_0^2 + 2\varepsilon D_0 D_1 + \varepsilon^2 D_1^2 \tag{25b}$$

where $D_0 = \frac{\partial}{\partial T}$, $D_1 = \frac{\partial}{\partial \tau}$.

Substituting (24) and (25) into (23) and equating the coefficients of the same power of ε gives

$$D_0^2 q_0 + k_1 q_0 = 0, \tag{26}$$

$$D_0^2 q_1 + k_1 q_1 = -(2D_0 D_1 + a_1 D_0 + k_2 p_1 \cos\bar{\Omega} T) q_0 - k_3 q_0^2 - k_4 q_0^3 \tag{27}$$

Obviously, the solution of (26) is

$$q_0 = A(\tau) e^{i\sqrt{k_1} T} + cc \tag{28}$$

where cc is the complex part conjugate to $A(\tau)e^{i\sqrt{k_1}T}$ and $i = \sqrt{-1}$. After inserting this solution into (27), it is found that principle resonance occurs at $\bar{\Omega} \approx 2\sqrt{k_1}$. To study the principle parametric resonance, and quantitatively describe the nearness of $\bar{\Omega}$ to two times of natural frequency, we define the detuning parameter σ

$$\bar{\Omega} = 2\sqrt{k_1} + \varepsilon\sigma \tag{29}$$

The condition below needs to be satisfied to eliminate the effect of long-term item

$$2i\sqrt{k_1}\frac{dA}{d\tau} + a_1 i\sqrt{k_1} A + 3k_4 A^2 \bar{A} + \frac{\bar{A}}{2} k_2 p_1 e^{i\sigma\tau} = 0 \tag{30}$$

where $\bar{A}$ is a complex number conjugate to A that can be expressed in polar coordinates

$$A(\tau) = R(\tau) e^{i\psi(\tau)} \tag{31}$$

Substituting (31) into (30) and separating the real and imaginary parts yields two equations to be used to determine $R(\tau)$ and $\psi(\tau)$

$$\frac{dR}{d\tau} + \frac{a_1 R}{2} + \frac{k_2 p_1 R}{4\sqrt{k_1}} \sin(\sigma\tau - 2\psi) = 0, \tag{32a}$$

$$R\frac{d\psi}{d\tau} - \frac{3k_4}{2\sqrt{k_1}} R^3 - \frac{k_2 p_1 R}{4\sqrt{k_1}} \cos(\sigma\tau - 2\psi) = 0 \tag{32b}$$

To find the equilibrium state in (32), set $\frac{dR}{d\tau} = 0$, $\frac{d\psi}{d\tau} = 0$ and one has

$$a_1^2 R^4 + \left(\sigma R^2 - \frac{3k_4}{\sqrt{k_1}} R^4\right)^2 = \frac{k_2^2 p_1^2 R^4}{4k_1} \tag{33}$$

Table 4 The first four linear frequencies of intact, clamped FGM beams

Frequency	$L/h = 15$		$L/h = 7$	
	Present	Ref. [37]	Present	Ref. [37]
ω_1	0.0287	0.0292	0.1241	0.1264
ω_2	0.0772	0.0786	0.3133	0.3184
ω_3	0.1468	0.1495	0.4567	0.4719
ω_4	0.2131	0.2205	0.5582	0.5675

This defines the relationship between excitation frequency and vibration amplitude.

Please note that both coefficients k_1 and k_3 represent the inhomogeneous material properties but due to the fact that the terms associated with k_3 do not contain long-term items, k_3 does not appear in (33).

6 Numerical results

Table 4 compares the present results and two-dimensional elasticity solutions [37] for the first four dimensionless linear frequencies $\omega = \Omega h\sqrt{(\rho/Q_{66})}$ of clamped FGM beams ($L/h = 7, 15$) with material parameters given in [37]. Good agreement is observed.

Table 5 lists the dimensionless fundamental frequencies ω_1/ω_{10} of clamped FGM beams with an open edge crack at different positions ($L_1/L = 0.0, 0.1, 0.2, 0.3, 0.4, 0.5$). ω_1 and ω_{10} denote the linear fundamental frequencies of the cracked and intact beams. The parameters used in this example are: $h = 0.1$ m; $a/h = 0.2$, $L/h = 10$; $E_2/E_1 = 0.2$, $E_1 = 70$ GPa; $\nu_1 = 0.33$, $\rho_1 = 2780$ kg/m^3. The beam is free from axial force. The present results agree well with those obtained using Euler–Bernoulli beam theory [33].

Unless otherwise stated, it is assumed in the following computations that the beam thickness $h = 0.1$ m, slenderness ratio $L/h = 6$; Young's modulus ratio $E_2/E_1 = 5.0, 1.0$, and 0.2. The beam is 100% aluminum at the top surface with the material parameters $E_1 = 70$ GPa; $\nu_1 = 0.33$; $\rho_1 = 2780$ kg/m^3. The static axial compressive force $P_0 = 0.8P_{cr}$ and P_{cr} is the critical buckling load. Crack depth $a/h = 0.0$ implies that the beam is intact and there is no edge crack in the beam. The deflection at mid-point of the beam is normalized as $W_0 = w/h$ in Tables 6, 7, 8 and Figs. 2–9.

Table 6 presents the dimensionless linear and nonlinear fundamental frequencies of clamped FGM

Table 5 Dimensionless fundamental frequencies ω_1/ω_{10} of clamped FGM beams with an edge crack

	$L_1/L=0.0$	$L_1/L=0.1$	$L_1/L=0.2$	$L_1/L=0.3$	$L_1/L=0.4$	$L_1/L=0.5$
Present	0.9255	0.9763	0.9992	0.9931	0.9755	0.9670
Ref. [33]	0.9427	0.9822	0.9994	0.9951	0.9822	0.9760

Table 6 Dimensionless linear and nonlinear fundamental frequencies of cracked FGM beams: Effect of crack location

L_1/L	$E_2/E_1=5.0$			$E_2/E_1=1.0$			$E_2/E_1=0.2$		
	Linear	Nonlinear		Linear	Nonlinear		Linear	Nonlinear	
		$W_0=0.4$	$W_0=0.8$		$W_0=0.4$	$W_0=0.8$		$W_0=0.4$	$W_0=0.8$
0.0	0.3897	0.4897	0.7055	0.4045	0.5024	0.7137	0.3837	0.4855	0.7027
0.1	0.3954	0.5011	0.7275	0.4132	0.5176	0.7449	0.3937	0.5049	0.7409
0.2	0.3978	0.5012	0.7237	0.4166	0.5170	0.7392	0.3979	0.5047	0.7340
0.3	0.3969	0.4913	0.6998	0.4154	0.5038	0.7021	0.3964	0.4859	0.6870
0.4	0.3957	0.4893	0.6952	0.4136	0.5020	0.6976	0.3942	0.4832	0.6828
0.5	0.3952	0.4879	0.6929	0.4129	0.5110	0.7144	0.3933	0.4825	0.6803

Table 7 Dimensionless linear and nonlinear fundamental frequencies of cracked FGM beams: Effect of crack depth

a/h	$E_2/E_1=5.0$			$E_2/E_1=1.0$			$E_2/E_1=0.2$		
	Linear	Nonlinear		Linear	Nonlinear		Linear	Nonlinear	
		$W_0=0.4$	$W_0=0.8$		$W_0=0.4$	$W_0=0.8$		$W_0=0.4$	$W_0=0.8$
0.0	0.3976	0.4974	0.7145	0.4164	0.5126	0.7239	0.3976	0.4977	0.7140
0.1	0.3957	0.4893	0.6952	0.4136	0.5020	0.6976	0.3942	0.4832	0.6803
0.3	0.3853	0.4492	0.5999	0.4005	0.4526	0.5794	0.3776	0.4231	0.5348
0.5	0.3704	0.4011	0.4787	0.3805	0.3930	0.4312	0.3516	0.3526	0.3576

beams with an open edge crack ($a/h=0.1$) at different locations. Table 7 gives the results for FGM beams containing an open edge crack at $L_1/L=0.4$ of various crack depths.

Numerical results show that the nonlinear fundamental frequency increases with an increase in vibration amplitude. The linear fundamental frequency of all beams is the minimum when the crack is located at the beam end ($L_1/L=0.0$). The graded beams with $E_2/E_1=5$ and $E_2/E_1=0.2$ have very close linear and nonlinear frequencies that are smaller than those of the homogeneous beam ($E_2/E_1=1$). Their nonlinear frequencies reaches the lowest value if the edge crack is at the midpoint of the beam ($L_1/L=0.5$) while for a homogeneous beam, the lowest nonlinear frequency is found at $L_1/L=0.4$. A deeper edge crack leads to a weaker cracked section thus results in lower linear and nonlinear frequencies. This effect, however, is much more pronounced for nonlinear frequencies. It is also observed from the results that the nonlinear frequency is significantly affected by crack depth, especially at higher vibration amplitudes, but is not very sensitive to the crack location. For example, the nonlinear fundamental frequency of the graded beam ($E_2/E_1=0.2$) drops by almost 48% as the crack depth increases from $a/h=0.1$ to $a/h=0.5$ while the biggest percentage difference between its fundamental frequencies with different crack location is less than 4%.

Table 8 compares the dimensionless linear and nonlinear fundamental frequencies of graded beams ($E_2/E_1=5.0$) with different slenderness ratio L/h ($=6, 10, 20$). The edge crack is located at $L_1/L=0.4$ and the crack depth is $a/h=0.3$. The linear and nonlinear frequencies become considerably lower as the slenderness ratio L/h changes from 6 to 20.

To compare the frequencies of FGM beams with and without an open edge crack, results for intact

Table 8 Dimensionless linear and nonlinear fundamental frequencies of cracked FGM beams: Effect of slenderness ratio

L/h	Linear	Nonlinear	
		$W_0 = 0.4$	$W_0 = 0.8$
6	0.3853	0.4492	0.5999
	0.3976*	0.4974*	0.7145*
10	0.2534	0.2956	0.3952
	0.2601*	0.3173*	0.4445*
20	0.1335	0.1575	0.2121
	0.1356*	0.1635*	0.2266*

beams are also provided in Tables 7 and 8 in which dimensionless linear and nonlinear frequencies at $a/h = 0.0$ in Table 7 and those with a superscript asterisk "$*$" in Table 8 are for intact FGM beams. Obviously, both linear and nonlinear natural frequencies of an intact beam are higher than those of a cracked beam, especially when the vibration amplitude is large and the slenderness ratio is small.

Figures 2, 3, 4 display the dynamic deflection responses of cracked FGM beams subjected to a harmonic axial excitation. Since the steady state response is much more important in engineering applications, deflection responses at $\bar{t} = 400 \sim 450$ are given while the results before $\bar{t} = 400$ are omitted in these figures. To study the principle parametric resonance, it is assumed that the excitation frequency is $\Omega = 0.85$, and the magnitude of dynamic force is $P_1 = 0.18, 0.085, 0.04$ for beams with $E_2/E_1 = 5.0, 1.0, 0.2$, respectively. The damping coefficient is taken to be $a_1 = 0.05$ as an illustrative example to include the damping effect on the nonlinear dynamic response.

Figure 2 shows the steady state responses of graded beams ($E_2/E_1 = 5.0$) with an edge crack ($a/h = 0.1$) at different locations ($L_1/L = 0.0, 0.1, 0.3, 0.5$). For beams containing an edge crack at the same location ($L_1/L = 0.3$), the effect of crack depth is studied in Fig. 3 where the steady state responses of an intact beam ($a/h = 0.0$) and cracked beams with $a/h = 0.1, 0.3$ are directly compared. To examine how the nonlinear dynamic behavior is influenced by material property gradient, Fig. 4 gives the steady state responses of intact beams and cracked beams ($L_1/L = 0.4, a/h = 0.3$) with Young's modulus ratio $E_2/E_1 = 5.0, 1.0, 0.2$. It is observed that the presence of edge crack increases the bending deflection of the beam and may also change the deflection response

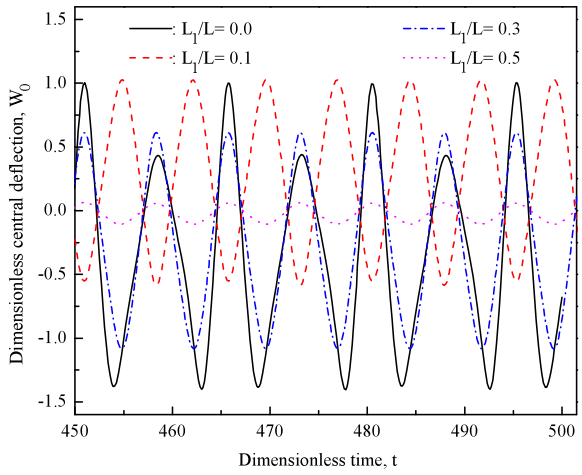

Fig. 2 Steady state responses of graded beams ($E_2/E_1 = 5.0$) with an edge crack ($a/h = 0.1$) at different locations

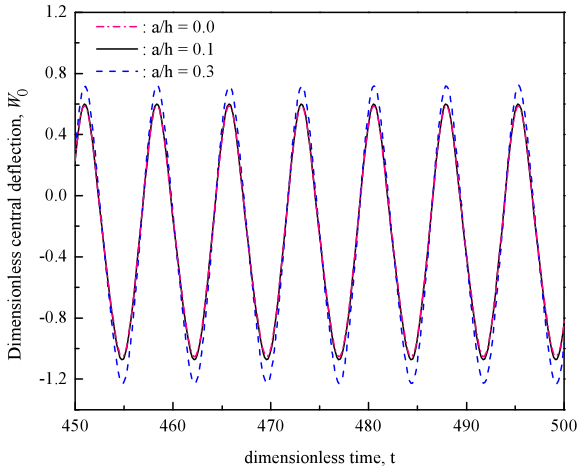

Fig. 3 Steady state responses of graded beams ($E_2/E_1 = 5.0$) with an edge crack ($L_1/L = 0.3$) of different depths

curve. As expected, vibration amplitude becomes significantly higher as the crack depth a/h increases due to the fact that the beam stiffness will be greatly weak-

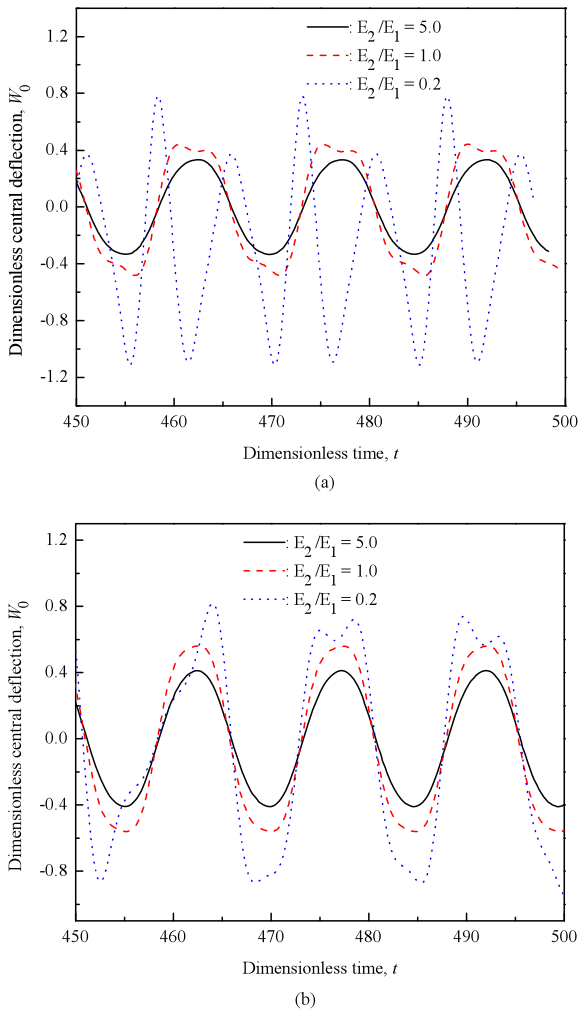

Fig. 4 Steady state responses of cracked FGM beams with different Young's modulus ratios: (**a**) intact beams; (**b**) cracked beams

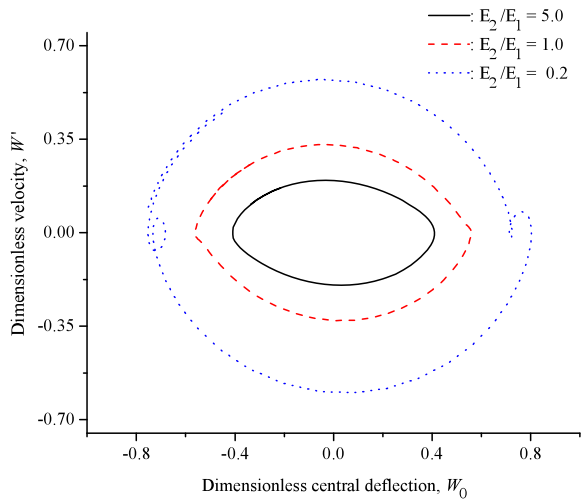

Fig. 5 Phase diagrams of cracked FGM beams ($L_1/L = 0.4$, $a/h = 0.3$) with different Young's modulus ratios

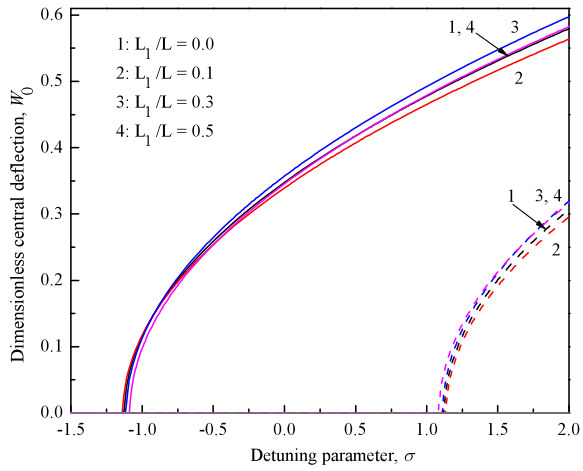

Fig. 6 Frequency responses of FGM beams ($E_2/E_1 = 5.0$) with an edge crack ($a/h = 0.1$) at different locations

ened by a deeper edge crack. The vibration amplitude is the maximum (minimum) when the crack is at the end (midpoint) of the beam but does not change very much as the crack moves from $L_1/L = 0.1$ to 0.3. The nonlinear central deflection is seen to increase as the Young's modulus E_2/E_1 decreases from 5.0 to 0.2. This is because the smaller the E_2/E_1 value is, the lower the bending stiffness of the beam becomes. It is also evident from Fig. 4 that the free vibration response already disappears at $\bar{t} = 400 \sim 450$ for intact and cracked beams with $E_2/E_1 = 5.0$ and 1.0 but still plays an important role in the total deflection response of the cracked beam whose Young's modulus ratio $E_2/E_1 = 0.2$.

Figure 5 presents the phase diagrams of FGM beams ($E_2/E_1 = 5.0, 1.0, 0.2$) with an edge crack ($a/h = 0.3, L_1/L = 0.4$) under a harmonic axial excitation ($P_1 = 0.04$). Results show that the beam with a smaller Young's modulus ratio is more flexible and has greater velocity as it vibrates. The phase diagram of the cracked beam with $E_2/E_1 = 0.2$ is different from and much more complicated than those of the other two cracked beams.

Figures 6, 7, 8, 9 investigate frequency responses, in form of dimensionless central deflection W_0 against the detuning parameter σ, of cracked FGM beams for various parameters. The solid lines and dashed lines

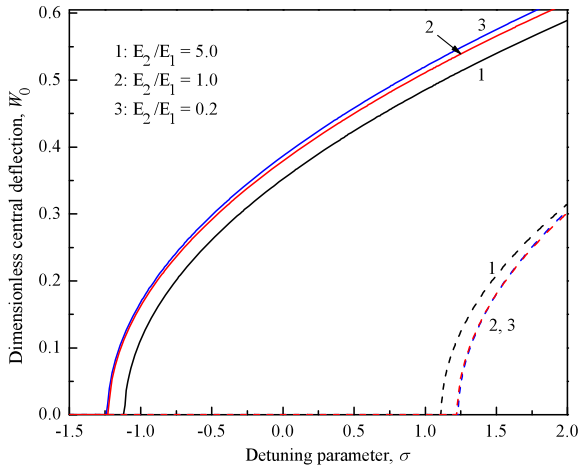

Fig. 7 Frequency responses of cracked FGM beams ($L_1/L = 0.3, a/h = 0.1$) with different Young's modulus ratios

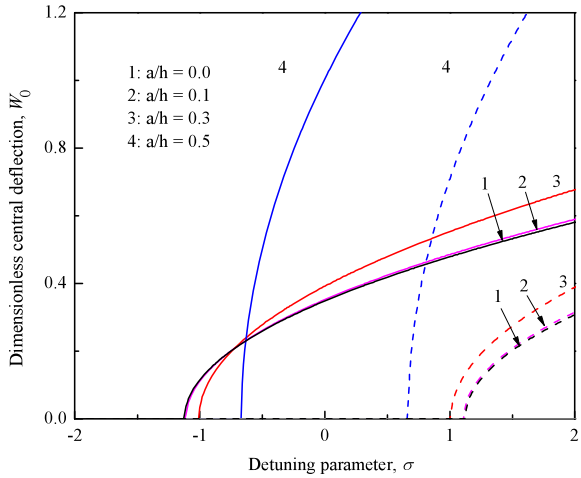

Fig. 8 Frequency responses of FGM beams ($E_2/E_1 = 5.0$) with an edge crack ($L_1/L = 0.3$) of different depths

represent the stable and unstable branches of the plots. All these branches bent to the right of each figure.

Plotted in Fig. 6 are the frequency-amplitude curves of a graded beam ($E_2/E_1 = 5.0$) with an edge crack ($a/h = 0.1$) at $L_1/L = 0.0, 0.1, 0.3$ and 0.5. Figure 7 shows the frequency responses of cracked beams ($a/h = 0.1, L_1/L = 0.3$) with different Young's modulus ratios ($E_2/E_1 = 5.0, 1.0, 0.2$). The effects of crack depth and slenderness ratio on the frequency responses are demonstrated in Figs. 8 and 9, respectively, where the results for intact beams are also provided. At the same crack depth and slenderness ratio, the branches of the frequency response curves

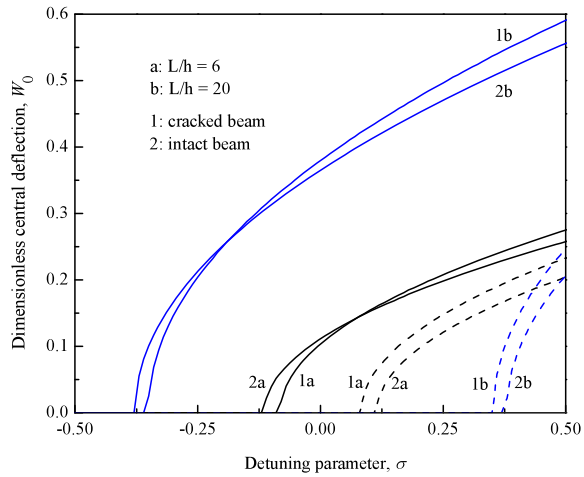

Fig. 9 Frequency responses of cracked FGM beams ($E_2/E_1 = 5.0, L_1/L = 0.4, a/h = 0.3$) of different slenderness ratios

converge to each other and the region between the branches becomes narrow as dimensionless central deflection and the Young's modulus ratio increase, as can be observed in Figs. 6 and 7. The frequency response curves, however, are insensitive to the change of crack location. It is also evident from Figs. 8 and 9 that the frequency-amplitude curves are considerably changed at different crack depths and slenderness ratios. Both the vibration amplitude and resonance region, especially the former, grow sharply at a large crack depth and slenderness ratio. These results are consistent with those presented in Figs. 2–5.

7 Concluding remarks

Nonlinear dynamic behavior of parametrically excited FGM Timoshenko beams containing an open edge crack is studied within the framework of Timoshenko beam theory, von Karman type nonlinear displacement-strain relationship, and rotational spring model. A parametric study has been conducted to examine how the nonlinear vibration frequency, steady state response and frequency-amplitude behavior are influenced by material property gradient, crack depth, crack location, and slenderness ratio. It is found that (1) the nonlinear natural frequency decreases as the crack depth and slenderness ratio increases and tends to be smaller when the crack is located at the beam end and the midpoint than at other places; (2) the steady

state deflection response becomes considerably higher as the crack depth increases and the Young's modulus ratio decreases. The dynamic deflection is the maximum (minimum) when the crack is at the beam end (midpoint); (3) FGM beams with a deep edge crack and large slenderness ratio have much higher vibration amplitude and bigger resonance region; (4) compared with other system parameters, crack location has a relatively small effect on the nonlinear dynamic behavior of parametrically excited FGM beams.

Appendix

In (23), let

$$J_{11}=\sin(\alpha\Delta),\quad J_{12}=\cos(\alpha\Delta),\quad J_{13}=\sinh(\beta\Delta),$$
$$J_{14}=\cosh(\beta\Delta),\quad J_{21}=\sin(\alpha),\quad J_{22}=\cos(\alpha),$$
$$J_{23}=\sinh(\beta),\quad J_{24}=\cosh(\beta),$$
$$Q_{11}=-m_1\alpha-\frac{n_1}{\alpha},\quad Q_{12}=-m_1\beta+\frac{n_1}{\beta},$$
$$Q_{21}=-m\alpha^3+n\alpha,\quad Q_{22}=m\beta^3+n\beta,$$
$$H_1=(e_{44}-p_0)\alpha-e_{44}Q_{21},$$
$$H_2=(e_{44}-p_0)\beta-e_{44}Q_{22},$$
$$f_{11}=-a_{11}Q_{11}+Q_{21}b_{11},$$
$$f_{12}=-a_{11}Q_{12}+Q_{22}b_{11},$$
$$f_{21}=-b_{11}Q_{11}+Q_{21}d_{11},$$
$$f_{22}=-b_{11}Q_{12}+Q_{22}d_{11}$$

the determinant in free vibration analysis for clamped-sliding FGM beams with single edge crack are given as below:

$$\bar{H}=\begin{vmatrix}
Q_{11} & 0 & Q_{12} & 0 & 0 & 1 & 0 & 0 & 0 & 0 & 0 & 0\\
0 & 1 & 0 & 1 & 0 & 0 & 0 & 0 & 0 & 0 & 0 & 0\\
Q_{21} & 0 & Q_{22} & 0 & 0 & 0 & 0 & 0 & 0 & 0 & 0 & 0\\
0 & 0 & 0 & 0 & 0 & 0 & f_{11}\alpha J_{21} & f_{11}\alpha J_{22} & -f_{12}\beta J_{23} & -f_{12}\beta J_{24} & a_{11} & 0\\
0 & 0 & 0 & 0 & 0 & 0 & J_{21} & J_{22} & J_{23} & J_{24} & 0 & 0\\
0 & 0 & 0 & 0 & 0 & 0 & Q_{21}J_{22} & -Q_{21}J_{21} & Q_{22}J_{24} & Q_{22}J_{23} & 0 & 0\\
Q_{11}J_{12} & -Q_{11}J_{11} & Q_{12}J_{14} & Q_{12}J_{13} & \Delta & 1 & -Q_{11}J_{12} & Q_{11}J_{11} & -Q_{12}J_{14} & -Q_{12}J_{13} & -\Delta & -1\\
J_{11} & J_{12} & J_{13} & J_{14} & 0 & 0 & -J_{11} & -J_{12} & -J_{13} & -J_{14} & 0 & 0\\
f_{11}\alpha J_{11} & f_{11}\alpha J_{12} & -f_{12}\beta J_{13} & -f_{12}\beta J_{14} & a_{11} & 0 & -f_{11}\alpha J_{11} & -f_{11}\alpha J_{12} & f_{12}\beta J_{13} & f_{12}\beta J_{14} & -a_{11} & 0\\
f_{21}\alpha J_{11} & f_{21}\alpha J_{12} & -f_{22}\beta J_{13} & -f_{22}\beta J_{14} & b_{11} & 0 & -f_{21}\alpha J_{11} & -f_{21}\alpha J_{12} & f_{22}\beta J_{13} & f_{22}\beta J_{14} & -b_{11} & 0\\
H_1J_{12} & -H_1J_{11} & H_2J_{14} & H_2J_{13} & 0 & 0 & -H_1J_{12} & H_1J_{11} & -H_2J_{14} & -H_2J_{13} & 0 & 0\\
f_{21}\alpha J_{11}-kQ_{21}J_{12} & f_{21}\alpha J_{12}+kQ_{21}J_{11} & -f_{22}\beta J_{13}-kQ_{22}J_{14} & -f_{22}\beta J_{14}-kQ_{22}J_{13} & 0 & 0 & kQ_{21}J_{12} & -kQ_{21}J_{11} & kQ_{22}J_{14} & kQ_{22}J_{13} & 0 & 0
\end{vmatrix}$$

References

1. Dimarogonas, A.D.: Vibration of cracked structures: a state of the art review. Eng. Fract. Mech. **55**(5), 831–857 (1996)
2. Gounaris, G.D., Papadopoulos, C.A., Dimarogonas, A.D.: Crack identification in beams by coupled response measurements. Comput. Struct. **58**(2), 299–305 (1996)
3. Lin, H.P., Chang, S.C., Wu, J.D.: Beam vibrations with an arbitrary number of cracks. J. Sound Vib. **258**(5), 987–999 (2002)
4. Khiem, N.T., Lien, T.V.: The dynamic stiffness matrix method in forced vibration analysis of multiple-cracked beam. J. Sound Vib. **254**(3), 541–555 (2002)
5. Wang, C.Y., Wang, C.M., Aung, T.M.: Buckling of a weakened column. ASCE J. Eng. Mech. **130**(11), 1373–1376 (2004)
6. Binici, B.: Vibration of beams with multiple open cracks subjected to axial force. J. Sound Vib. **287**(1–2), 277–295 (2005)
7. Caddemi, S., Calio, I.: Exact solution of the multi-cracked Euler–Bernoulli column. Int. J. Solids Struct. **45**(5), 1332–1351 (2008)
8. El Bikri, K., Benamar, R., Bennouna, M.M.: Geometrically non-linear free vibrations of clamped–clamped beams with an edge crack. Comput. Struct. **84**(7), 485–502 (2006)
9. Kisa, M., Brandon, J., Topcu, M.: Free vibration analysis of cracked beams by a combination of finite elements and component mode synthesis methods. Comput. Struct. **67**(4), 215–223 (1998)
10. Zheng, D.Y., Fan, S.C.: Natural frequency changes of a cracked Timoshenko beam by modified Fourier series. J. Sound Vib. **246**(2), 297–317 (2001)
11. Loya, J.A., Rubio, L., Fernández-Sáez, J.: Natural frequencies for bending vibrations of Timoshenko cracked beams. J. Sound Vib. **290**(3–5), 640–653 (2006)
12. Nayfeh, A.H., Pal, P.F.: Nonlinear non-planar parametric responses of an inextensional beam. Int. J. Non-Linear Mech. **24**(2), 138–158 (1989)
13. Zavodney, L.D., Nayfeh, A.H.: The nonlinear response of a slender beam carrying a lumped mass to a principal parametric excitation: theory and experiment. Int. J. Non-Linear Mech. **24**(2), 105–125 (1989)
14. Abou-Rayan, A.M., Nayfeh, A.H., Mook, D.T., Nayfeh, M.A.: Nonlinear response of a parametrically excited buckled beam. Nonlinear Dyn. **4**, 499–525 (1993)

15. Kar, R.C., Dwivedy, S.K.: Nonlinear dynamics of a slender beam carrying a lumped mass with principal parametric and internal resonances. Int. J. Non-Linear Mech. **34**(3), 515–529 (1999)
16. Anderson, T.J., Nayfeh, A.H., Balachandran, B.: Experimental verification of the importance of the nonlinear curvature in the response of a cantilever beam. ASME J. Vib. Acous. **118**(1), 21–27 (1996)
17. Delale, F., Erdogan, F.: The crack problem for a nonhomogeneous elastic medium. ASME J. Appl. Mech. **50**(3), 609–614 (1983)
18. Noda, N., Jin, Z.H.: A crack in functionally gradient materials under thermal shock. Arch. Appl. Mech. **64**(2), 99–110 (1994)
19. Jin, Z.H., Batra, R.C.: Some basic fracture mechanics concepts in functionally graded materials. J. Mech. Phys. Solids **44**(8), 1221–1235 (1996)
20. Erdogan, F., Wu, B.H.: The surface crack problem for a plate with functionally graded properties. J. Appl. Mech. ASME **64**(3), 448–456 (1997)
21. Praveen, G.N., Reddy, J.N.: Nonlinear transient thermoelastic analysis of functionally graded ceramic-metal plates. Int. J. Solids Struct. **35**(33), 4457–4476 (1998)
22. Yang, J., Shen, H.S.: Dynamic response of initially stressed functionally graded rectangular thin plates resting on elastic foundations. Compos. Struct. **54**(4), 497–508 (2001)
23. Yang, J., Shen, H.S.: Free vibration and parametric resonance of shear deformable functionally graded cylindrical panels. J. Sound Vib. **261**(5), 871–893 (2003)
24. Yang, J., Liew, K.M., Kitipornchai, S.: Dynamic stability of laminated FGM plates based on higher-order shear deformation theory. Comput. Mech. **33**(4), 305–315 (2004)
25. Huang, X.L., Shen, H.S.: Nonlinear vibration and dynamic response of functionally graded plates in thermal environments. Int. J. Solids Struct. **41**(9–10), 2403–2427 (2004)
26. Sundaraja, N., Prakash, T., Ganapathi, M.: Nonlinear free flexural vibration of functionally graded rectangular and skew plates under thermal environments. Finite Elem. Anal. Des. **42**(2), 152–168 (2005)
27. Yang, J., Liew, K.M., Wu, Y.-F., Kitipornchai, S.: Thermo-mechanical post-buckling of FGM cylindrical panels with temperature-dependent properties. Int. J. Solids Struct. **43**(2), 323–340 (2006)
28. Yang, J., Liew, K.M., Kitipornchai, S.: Second-order statistics of the elastic buckling of functionally graded rectangular plates. Compos. Sci. Technol. **65**(7–8), 1165–1175 (2005)
29. Hao, Y.X., Chen, L.H., Zhang, W., Lei, J.G.: Nonlinear oscillations, bifurcations and chaos of functionally graded materials plate. J. Sound Vib. **312**, 862–892 (2008)
30. Zhang, W., Yang, J., Hao, Y.X.: Chaotic vibration of orthotropic FGM rectangular plates based on the third-order shear deformation theory. Nonlinear Dyn. **59**(4), 619–660 (2010)
31. Sridhar, R., Chakraborty, A., Gopalakrishnan, S.: Wave propagation analysis in anisotropic and inhomogeneous uncracked and cracked structures using pseudospectral finite element method. Int. J. Solids Struct. **43**(16), 4997–5031 (2006)
32. Yang, J., Chen, Y., Xiang, Y., Jia, X.L.: Free and forced vibration of cracked inhomogeneous beams under an axial force and a moving load. J. Sound Vib. **312**(1–2), 166–181 (2008)
33. Yang, J., Chen, Y.: Free vibration and buckling analyses of functionally graded beams with edge cracks. Compos. Struct. **83**(1), 48–60 (2008)
34. Ke, L.L., Yang, J., Kitipornchai, S., Xiang, Y.: Flexural vibration and elastic buckling of a cracked Timoshenko beam made of functionally graded materials. Mech. Adv. Mat. Struct. **16**(6), 488–502 (2009)
35. Yang, J., Hao, Y.X., Zhang, W., Kitipornchai, S.: Nonlinear dynamic response of a functionally graded plate with a through-width surface crack. Nonlinear Dyn. **59**(1–2), 207–219 (2010)
36. Broek, D.: Elementary Engineering Fracture Mechanics. Martinus Nijhoff, Dordrecht (1986)
37. Lu, C.F., Chen, W.Q.: Free vibration of orthotropic functionally graded beams with various end conditions. Struct. Eng. Mech. **20**(4), 465–476 (2005)